MANAGEMENT OF FLUID INJECTION IN GEOTHERMAL WELLS TO AVOID SILICA SCALING AT LOW LEVELS OF SILICA OVERSATURATION

Christopher W. Klein

Geothermex, Inc., 5221 Central Avenue, Suite 201, Richmond, California 94804, **USA**

Key Words: scaling, silica, rate. modeling, prediction, injection

ABSTRACT

In the design of geothermal installations, the possibility of scale precipitation caused by silica oversaturation has often been taken as a design constraint upon steam separation pressure. At installations where oversaturation is allowed to develop, the resulting scale formation is a nuisance and in some cases affects the performance of injection wells. **A** review of the thermodynamics, reaction mechanisms, and kinetics of silica deposition, compared with actual experience at various locations, shows that it is possible to predict low-level scaling with sufficient confidence for production and injection system design. With foresight it thus becomes possible to suppress or manage the silica scale. A useful suppression technology is fluid pH reduction, achieved by mixing with non-condensible gases and/or steam condensate. Results from several geothermal systems will be presented. Further improvements of predictive technique will benefit from more uniformity in data collection, designing experiments, reporting of results, and reporting measurements of scaling in actual production systems.

1. INTRODUCTION

In spite of industry success in learning to manage the severe scaling from hypersaline geothermal brines in the Salton Sea area **of** California, USA, scaling from low levels of oversaturation in more typical, lower salinity waters remains a nuisance. The pressure/temperature at which a boiling wellflow saturates with amorphous silica is generally used to constrain the design of production conditions. When oversaturation occurs, typical scale management includes: 1) periodic clean-out or replacement of separators and pressurized disposal lines, and (2) flashing to atmospheric pressure so that silica can be driven out of solution and removed by chemical/mechanical means (*e.g.*, flocculation and settling) before the residual brine is injected back into the reservoir. Where the oversaturation of pressurized brine is not too severe, direct injection may be practiced. However, silica scale is often the inferred cause of mild to severe permeability losses in injection pipelines and wells.

Because silica scaling mechanisms are fairly complex and poorly quantified, it has been common to manage scale on the basis of local field experiments. However, comparisons of the results of such studies (published and unpublished) are hindered by a lack of uniformity in experimental design, methodology and reporting. This paper addresses the nature of the scaling mechanism, and shows that it is generally possible to predict low-level scaling with sufficient confidence for production and injection system design. With foresight, it thus becomes possible to suppress or manage the scale. Recommendations are also presented, for more uniformity in designing experiments, reporting results, and reporting measurements **of** scaling in actual production systems.

2. SCALING MECHANISMS

When reservoir water boils and loses steam through a pressure drop, silica saturation can be simply calculated using a graphical solution (figure 1). The figure shows the solubilities of quartz (Fournier and Potter, 1982), chalcedony (Fournier, 1981 and Arnorsson *et al.*, 1983), and amorphous silica (Fournier, 1981; Chen and Marshall, 1982; Fournier and Marshall, 1983) in water with pH below about 8 and at the enthalpy of steam saturation. Adjustments to the solubility curves can be made when pH is high (*e.g.*, Henley, 1983; also, see below). **A** straight line passes through two known points (steam at separation pressure and conditions in the reservoir) and leads to the silica concentration in the residual liquid. Figure 1 shows the case of a 3 month flow test at the Uenotai field in Japan (Klein, *et al.*, 1991). At the wellhead conditions of **4** bar/ 142°C, there was 340 mg/kg oversaturation with amorphous silica, and a thick deposit of soft white scale formed on the control valve. The fluid represented on figure 1 is listed in Appendix A.

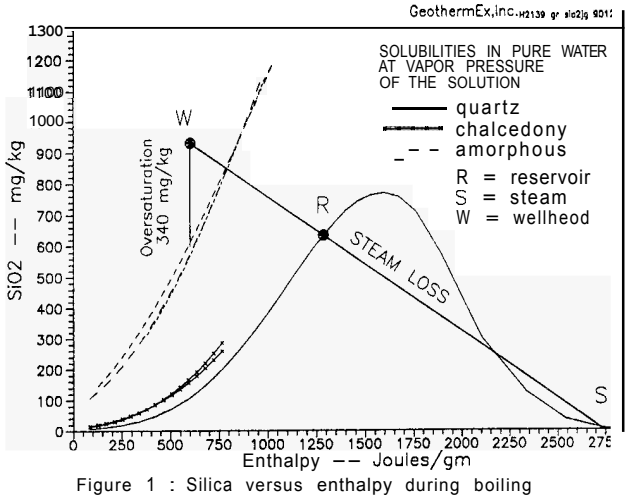

Figure 1 : Silica versus enthalpy during boiling

A complete review of silica chemistry with respect to over-saturation is beyond the scope of this paper, but a summary of the most essential and satisfactory theory is needed. Major bibliographies are provided by Marsh *et al.* (1975), Iler (1979) and Chan (1989).

In solution, the dissolved silica, which is usually reported **as** SiO_2, behaves as a molecule named silicic acid, written $Is(OH)_4^o$ or $H_4SiO_4^o$. This can be described as a combination of SiO_2 with two water molecules. More essential is the concept that it contains four separate -OH groups bonded to a central Is atom:

OH
HO-Is-OH
OH

These four "silinol" groups have two essential behaviors; one is acidity. A silinol group can lose its proton (H^+), although silicic acid is weak and therefore insignificantly ionized at low pH. The loss of one proton produces silicate ion:

$$H_4SiO_4^\circ = H_3SiO_4^- + H^+.$$

At 25°C, the proportion of silicate ion to unionized silica ($H_3SiO_4^-/H_4SiO_4^\circ$) is about 1/100 at pH 7.8, 1/10 at pH 8.8, and 1/1 at pH 9.8. Heating from 25°C to about 175°-200°C causes acidity to increase by about an order of magnitude, so that the silicate/silicic acid ratio is 1/1 at about pH 8.8; it then decreases again as temperature rises further. $H_2SiO_4^=$, which forms when a second proton is lost, remains nearly insignificant except at very high pH. Some $H_3SiO_4^-$ is conventionally considered to combine with Na+ to form dissolved sodium silicate, $NaH_3SiO_4^\circ$.

The second behavior is reactions between silinol groups to form the Is-0-Si bonds in silica minerals. When there is chemical equilibrium or an approach to equilibrium, these reactions combined with the acid dissociation determine the maximum undissociated $H_4SiO_4^\circ$ in a solution at a given temperature. Solution composition has some effect on these processes, whereas pressure has little effect except at extremely high levels.

Reservoir water at thermodynamic equilibrium typically contains $H_4SiO_4^\circ$ in a concentration determined by the least soluble solid silica phase, which is pure SiO_2 as quartz. Below about 180°C, quartz tends to develop in a particular crystal morphology called chalcedony, which has somewhat higher solubility (figure 1). When a quartz-saturated solution oversaturates by boiling, it rarely forms quartz scale unless temperature remains above about 220°C, because the rate of crystal growth is extremely slow relative to wellbore processes.

A boiling and/or cooling solution can eventually oversaturate with silica to the point where $H_4SiO_4^\circ$ becomes limited by Is-0-Si bonding into polymers. The initial step in this process is a "condensation reaction", between the silinol groups on two silicic acid molecules, when one of the two groups is ionized (Marsh *et al.*, 1975):

$$H_4SiO_4^\circ + H_3SiO_4^- = H_6Si_2O_7^\circ + OH^-, \text{ or}$$

$$\begin{array}{ccccc} OH & & OH & & OH\ OH \\ HO\text{-}Is\text{-}OH & + & {}^-O\text{-}Is\text{-}OH & = & HO\text{-}Is\text{-}0\text{-}Si\text{-}OH \\ OH & & OH & & OH\ OH \end{array} + OH^-$$

Deposition onto an iron surface can begin by an analogous process, where dissolved silicic acid reacts with an -OH group on corroded iron.

Compared to quartz crystals, the growing polymers are chaotic, with irregular surfaces, numerous remaining silinol groups, and infinitely branching structures. However, they equilibrate with a predictable concentration of dissolved SiO_2 which defines the solubility of amorphous silica (figure 1). It is common to express this solubility as SiO_2 and refer to it as the concentration of monomeric silica (also termed m-SiO_2) or $H_4SiO_4^\circ$, and this terminology is used herein. However, the soluble silica actually is a mixture of low molecular weight silicic acids (monomer, dimer, trimer; Marsh *et al.*, 1975).

The solubility of any silica solid (quartz, chalcedony, amorphous silica) is conventionally expressed as the concentration of unionized silica in solution. Any ionized silica which is present exists in addition to $H_4SiO_4^\circ$; so as a consequence, the total SiO_2 in solution (T-SiO_2 = unionized SiO_2 + ionized SiO_2) increases as pH increases. This is sometimes called apparent solubility, as opposed to the true solubility when ionized SiO_2 is not present. Figure 2 shows the difference between total SiO_2 and SiO_2 in $H_4SiO_4^\circ$ during boiling of the geothermal well fluid which is listed in Appendix A, with solubility plotted versus temperature instead of enthalpy. The relevant calculations are described in Appendix B.

Fluid pH also exerts significant control on polymerization rate. The causes of this are not completely understood, but implied by the condensation reaction as written above. Since polymers grow by collision of an unionized -OH unit with an ionized -O^- unit, polymerization rates should be at a maximum when the concentrations of available -OH and -O^- on growth surfaces are equal. In a slightly oversaturated solution, this is the pH at which $H_4SiO_4^\circ = H_3SiO_4^-$ (pH 9.8 at 25°C; 8.8 at 175°-200°C, see above). Large polymers have higher acidity, so a strongly oversaturated solution can exhibit its maximum growth rate at somewhat lower pH.

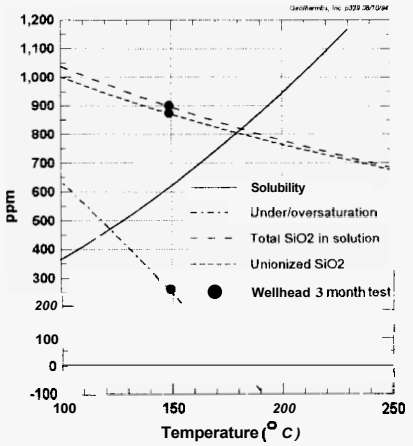

Figure 2 Silica species and saturation of amorphous silica dunng boiling of example fluid (figure 1 and Appendix A)

The pH effect generally is observed, and as an approximate rule lowering the solution pH slows kinetics by a factor of about 10 for every pH unit (*e.g.*, Rothbaum *et al.*, 1979; Hirowatari and Yamaguchi, 1990).

In an oversaturated solution, the relationship between polymer growth and actual scale deposition is a function of combined chemical and physical processes which follow two dominant and essentially competing pathways: molecular deposition and particle deposition.

Molecular deposition occurs when the growing polymer surface is a solid, to which silicic acid and silicate ions migrate by circulation and diffusion. The rate of deposition is a function of temperature, supersaturation, and the density of silinol groups ionized to -Is-O^- on the solid growth surface. The effective surface density increases with salinity and, of course, pH (Weres *et al.*, 1982). This rate is discussed further below.

Particle deposition follows nucleation and growth of suspended polymers. The starting process is termed homogeneous nucleation because the polymers develop spontaneously in solution and not by deposition onto foreign particles or ions of other solutes. This is a chemically reversible process. It starts with an "induction period' which proceeds smoothly, on a logarithmic time scale, into a period of rapid polymer growth, then slowing growth as the oversaturation of the solution is depleted. At low levels of oversaturation (and/or low pH), the induction period can last minutes to hours. When initial supersaturation exceeds about 2 to 2.5, the induction period often is instantaneous, and polymer growth very rapid.

Many studies of induction period and polymerization rate have been published (*e.g.*, see Kindle *et al.*, 1974; Hurtado and Mercado, 1990; and Thordarson and Tomasson, 1989). However, it must be considered that such studies typically are context specific, depending strongly on SiO_2 concentration, temperature, salinity and pH. Induction will be shorter at higher SiO_2; for a given SiO_2 level, induction will be shorter at

lower temperature, higher salinity, and higher pH, except when counteracted at very high pH by increased solubility. Marsh *et al.* (1975) also note that many studies of polymerization rate have been flawed by inadequate experimental technique and misinterpretation of results. Weres *et al.* (1982) have discussed a computer program for calculation of nucleation rates (see below).

The properties of the growing polymers, such as individual size and acidity, change continuously as they grow, and different solutions mature differently. For example, the relatively low nucleation rates at high temperatures cause formation of fewer particles which tend eventually to become larger. At low temperature there typically is a higher supersaturation ratio, and nucleation produces larger numbers of smaller particles. High pH causes rapid growth of many particles which aggregate quickly into larger units, whereas low pH promotes the continued separate growth of smaller particles.

There is a loosely defined size (usually termed "critical size") above which the growing polymers are considered to be colloidal particles. At this point they are spherical in shape, and once greater than about 10nm in diameter, they apparently grow by molecular deposition at the same rate as surface scale. There is competition between surface scale and suspended particles for the supply of excess $Is(OH)_4$ in solution. Therefore, when the particles are abundant and growing, the rate of molecular deposition onto solid surfaces (*e.g.*, pipe walls) may decrease, because the particles are taking $Is(OH)_4$ out of solution.

The colloidal particles can deposit as scale when they reach solid surfaces, driven by diffusion, flow turbulence, and sometimes gravity. If these transfer processes are rapid, scale can grow on the surface much more rapidly than it could by molecular deposition alone. Mass transfer tends to be most rapid at low temperature, when particle sizes are small, and at high turbulence. Adhesion of particles onto solid surfaces appears to be both a chemical and a physical process; once adhered, the particles can become cemented by further molecular deposition. In static or slowly flowing regimes, the scaling process can be affected further by coagulation or flocculation of colloidal particles to give either a precipitate or a suspended semi-solid material, or a gel; some solutions form stable colloids which do not precipitate.

Molecular deposition is primarily responsible for producing hard, vitreous, often dark colored scale, with density about 2.1 to 2.3 g/cc. In contrast, particle deposition produces white, fluffy, scale with dry density about 0.95 g/cc. Exceptions to these rules have been described, including hard scale believed to have deposited by particle deposition, and soft white scale which formed at low oversaturation within the expected induction period (Jamieson, 1984). Changes in flow rates or supersaturation may be marked by alternating laminae of vitreous and fluffy scale. In pipelines, the scale often forms radial ridges transverse to the flowpath, which can cause considerable roughness to fluid flow (*e.g.*, Stock, 1990).

3. SCALING EXPERIENCE

Published and informal reports of scaling experience generally are very difficult to compare and evaluate in light of the processes described above, because there is a lack of standards in reporting. The number of published reports is fairly small, and descriptions are typically incomplete (see recommendations below), but most allow some illustration of scaling rate or effects in relation to temperature or pressure and SiO_2 concentration. Klein *et al.* (1991) presented a detailed summary of experience at Cerro Prieto, Mexico; Dixie Valley, Nevada, **USA,** Milos, Greece; Otake and Hatchobaru, Japan; Svartsengi, Iceland; and the experimental results of Mroczek and McDowell (1990). The quantitative data obtained from this work are further summarized herein as figure 3, which shows observed scaling rates from unaltered brine at the approximate concentration of unionized, monomeric SiO_2 in solution.

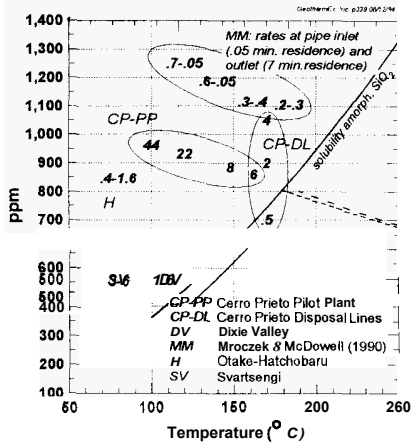

Figure 3 Summary of scaling experience showing rates in mm/yr at approximate temperature (see text) Reference curves are from figure 2

Excepting the data of Mroczek and McDowell (1990), the scaling represented on figure 3 is dominantly by particle deposition, and the particle deposition rates are highly variable. The Cerro Prieto pilot plant results may be the effect of excessive turbulence, which enhances the particle deposition rate. Turbulence would also explain the abundance of scale at the control valve of the well represented in figure 1 (not plotted in figure 3 because deposition rate was not reported). In contrast, the lower rates at Dixie Valley and Svartsengi were measured in injection disposal lines, where the flow regimes probably were more homogeneous, as also in the Cerro Prieto disposal lines. (In addition, Dixie Valley scale contains *6%* to 12% Al_2O_3 (Dick Benoit, oral communications.), which undoubtedly has an effect on solubility and reaction rates.) Scale formation from the Hatchobaru brine was measured in a pilot apparatus, but the published description of rate was sketchy, and the scale morphology was not described. The slow rate implies molecular deposition. Considering these observations, it appears that oversaturation below about 150ppm is unlikely to produce particulate scale at a rate exceeding *2* or 3 mm/yr, as long as excessive turbulence is avoided. Against this the molecular deposition data of Mroczek and McDowell (1990) provide a lower limit.

The well-controlled and documented experimental work of Mroczek and McDowell (1990) was conducted by passing separated brine from a well through a pipeline for 29 to 35 days. Then the pipeline was cut into even sections and the amount of scale in each section determined. Eight experiments were run, two each with separator pressure set for 180°C, 160°C, 140°C and 120°C. At each pressure there was one experiment with a brine flowrate of 3 l/sec, and another with a rate of 30 l/sec; this produced total residence times of 7 minutes and 0.7 minutes. Total SiO_2 and monomeric SiO_2 were measured in water samples collected ai the inlet and outlet. Salinity and pH were not reported, but saturation ratios and T-SiO_2 values suggest that there was essentially no ionized silica.

At 180°Cand 160°C, the induction time for polymerization was not reached, even at 7 minutes. Scaling rates were 0.2 to 0.3 mm/yr at 180°C (assuming density 2.2), increasing to 0.3 to 0.4 mm/yr at 160°C. At 140°Cand 120°C, there was measurable polymer formation, even at the pipe inlet, and the polymer concentration increased through the pipeline; the increase at 120°C was twice that at 140°C. Therefore, scaling in the pipeline decreased dramatically along the length of the pipe, as monomeric SiO_2 was removed from solution into the suspended polymer. In all cases, the scale which formed was hard and glassy, with density about 2 gm/cc.

Mroczek and McDowell (1990) also performed some tests of silica deposition using gravel beds substituted for the open pipeline. Results were imprecise because the mass of silica deposited proved hard to measure. However, at 180°C and 160°C, there was a hard silica scale which deposited uniformly along the length of the beds. At 140°C and 120°C, there were soft, loosely adhering deposits at the bed inlet, with hard deposits downstream at 140°C, but no deposits elsewhere at 120°C. The bed inlet was a point of high flow rate and turbulence.

4. KINETIC STUDIES

Weres *et al.* (1982) studied polymerization and particle growth in aqueous solutions up to 100°C and containing up to 1 M NaCl (35,000 pprn Cl), to obtain rate equations for homogeneous nucleation and molecular deposition. This work produced graphs and equations for calculating molecular deposition rate and suspended particle growth rate. Jamieson (1984) has published some general mathematical relationships which describe the rate of mass transfer of particles from suspension in flowing solutions to surrounding solid surfaces. However, these have not yet been integrated with expressions for particle nucleation and growth, and calculations of particle scaling rates are not yet routinely possible.

Figure 4 (after Weres *et al.*, 1982) shows rates of molecular deposition versus temperature and the concentration of unionized SiO_2 at a pH of 7 and NaCl salinity equivalent to about 2,400 ppm Cl. Corrections for different pH or salinity can be calculated. The quadrilateral outline on figure 4 corresponds to experimental data; rate lines outside this area were calculated. The dotted line connects points of maximum rate at given SiO_2.

Weres *et al.* (1982) have cautioned that figure 4 and their rate equations should not be overused for scaling predictions. Their experimental data were collected at relatively low temperature, by adding known amounts of colloidal silica of known surface area to oversaturated solutions, and monitoring the loss of monomeric SiO_2. This process presented to their silica solutions a widely dispersed area of curved surfaces; thus, their experimental conditions were different from scale deposition on the wall of a pipe.

The work of Mroczek and McDowell (1990) suggests, however, that under the right conditions a prediction can be quite accurate. The predicted points for Mroczek and McDowell on figure 4 are plotted simply at total SiO_2 and temperature; measured points are plotted at temperature and observed rate. There is excellent agreement at 120°C, good agreement at 140°C, and progressively poorer agreement at 160°C and 180°C, with the predicted rates exceeding those actually observed.

Molecular deposition rates predicted for Dixie Valley and for the example fluid of Appendix A and figure 1 are one to two orders of magnitude lower than the particle deposition rates actually observed.

5. EXAMPLE OF DEVELOPING A PREDICTION OF SCALING RATE

An example of scaling rate prediction can be provided by consuturing the fluid of Appendix A under proposed production conditions. Chemical modeling (Appendix B) indicates saturation with amorphous silica at 10.8 bar/182°C. If production separation is at 9.3 bar/175°C, where total SiO_2 = 850 ppm, pH = 7.2, Cl = 225 ppm, then there will be 70 ppm oversaturation and saturation ratio of 1.1. Suppose also that the fluid is maintained at separation pressure and temperature throughout the injection system, and maximum pipeline residence time is 20 to 45 minutes.

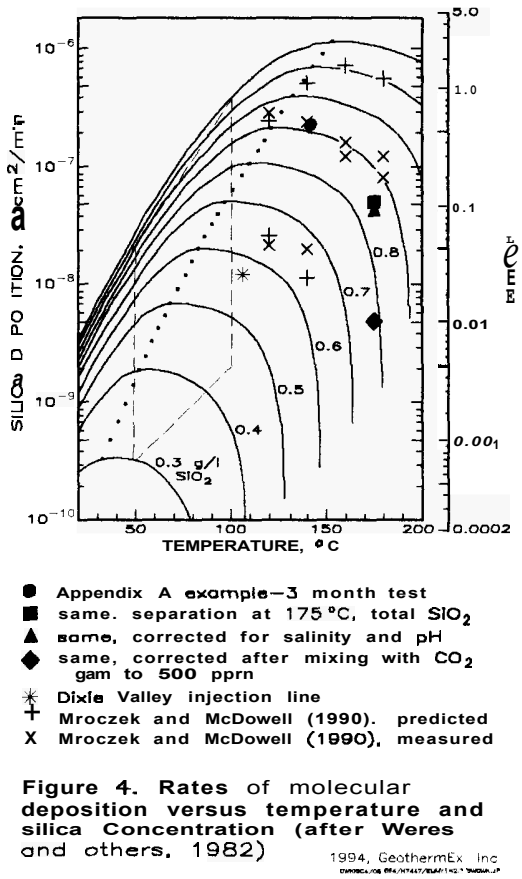

Figure 4. Rates of molecular deposition versus temperature and silica Concentration (after Weres and others, 1982)

These conditions indicate molecular deposition at about 0.1 to 0.15 mm/yr (figure 4), although this figure is approximate. Furthermore, it is expected that molecular deposition will be more significant as a scaling mechanism than particle deposition, because pH and salinity will not be particularly high, residence time will be relatively short, and supersaturation ratio low. The indicated oversaturation is below the range applicable to the homogeneous nucleation rate equations of Weres *et al.* (1982), which prompts their guideline that molecular deposition should be dominant. Furthermore, a comparison with nucleation rate curves for higher oversaturation (Weres *et al.* (1982)) furthermore indicates that the induction period will not be reached.

The experimental evidence of Mroczek and McDowell (1990) suggests that scaling rates will be nearly uniform along the length of the injection pipelines, with some extra build-up possible at points of turbulence. The scale is more likely to be hard than soft. Soft scale which does develop is likely to be fairly rough, forming radial ridges transverse to pipeline flow, which cause impedance. A conservative interpretation of the general experience with injection lines elsewhere indicates that some scale should be considered probable, but not likely at rates exceeding 1 mm/yr to 2 mm/yr. Therefore, a strategy to suppress or manage the expected scale can be recommended.

6. SUPPRESSION BY GAS OR CONDENSATE MIXING

Gas mixing to lower solution pH and suppress scale development has been discussed by Hirowatari and Yamaguchi (1990). Figure 5 is a model of dissolving various amounts of CO_2 into the injection line brine, after separating the brine from steam at 175°C. The particular case modeled starts at 50 ppm oversaturation. Between 25 ppm and 500 ppm total C in solution as CO_2, there is a dramatic drop of pH from 7.2 to 5.8, while unionized SiO_2 climbs from 822 ppm to 850 ppm and oversaturation increases from 50 ppm to 75 ppm. The increase of oversaturation is completely counterbalanced by the lowered pH, and molecular deposition

rate drops from 0.15 to 0.01 mm/yr (figure 4). This should also effectively eliminate any tendency for particle formation and deposition. pH and scaling potential can be lowered further with additional CO_2, but this hardly seems necessary. It should be noted that P_{CO2} for 500 ppm is only 1.5 bar. The 500 ppm level is achieved by mixing about 0.025 t/hr non-condensible gases (13 m^3 at 1 atm.) per 50 t/hr of water flow.

For comparison with the gas mixing, we note the following: 1) mixing 50 t/hr water flow with 17.5 t/hr condensate at 60°C also lowers the molecular deposition rate to 0.01 mm/yr; 2) all oversaturation in 175°C water would be removed by mixing with an equal amount of 60°C condensate; and 3) mixing with a combination of gas and condensate may have a beneficial effect by reducing wintertime freezing of vapor in the gas line.

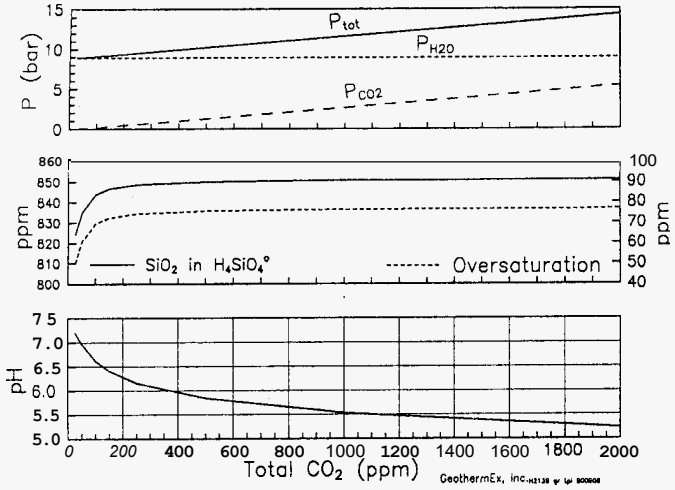

Figure 5. Effect of mixing CO, into water fraction at 175°C, Appendix A example fluid

7. MANAGEMENT STRATEGIES

In addition to scale suppression strategies, the following is recommended for scale management at low levels of oversaturation:

1) Design the injection system to minimize residence time and avoid turbulence.

2) Install pressure ports on injection lines to allow monitoring for scale-related impedance.

3) Install inspection ports and scaling coupon ports on the injection lines.

4) Install ports at both ends of injection lines to allow inserting a clean-out pig.

8. RECOMMENDATIONS FOR DATA GATHERING

It is clear from a literature review that further improvements of predictive technique will benefit from more uniformity in designing experiments, reporting results, and reporting descriptions of scale. We strongly recommend that the following be included in all reports of silica scale in production systems, pilot plants, or experimental systems:

Complete chemical analysis of the major elements and pH in the scale-forming water, collected at an upstream sample point.

2) Temperature, total SiO_2, monomeric SiO_2 (by colorimetry), and pH (with sample temperature) at upstream and downstream sample points. The technique of sampling and colorimetric measurement must be researched and applied carefully to give reliable results.

3) Complete analyses of the major elements and gas species in a separated water and steam sample suite, including pH, total flow enthalpy and separation pressure/temperature. The purpose of this is to allow modeling the fluid at different pressures and temperatures.

4) A short but considered description of scale morphology vis-a-vis the probable dominance of molecular deposition or particle deposition.

5) A description of scale thickness and location vis-a-vis uniformity and flow turbulence.

6) A description of scaling rate, or total period of fluid flow in relation to scale mass or thickness. Rates should be reported both in mg/area/time and mm/yr with scale density.

7) A description of system volume and flow rate, or fluid residence time.

9. REFERENCES

Amorsson, S., and S. Sigurdsson, 1982. The chemistry of geothermal waters in Iceland I: Calculation of aqueous speciation from 0" to 370°C. Geochimica et Cosmochimica Acta, Vol. 46, pp. 1513-1532.

Amorsson, S., E. Gunnlaugsson, and H. Svavarsson, 1983. The chemistry of geothermal waters in Iceland III: Chemical geothermometry in geothermal investigations. Geochimica et Cosmochimica Acta, Vol. 47, pp. 567-577.

Chan, S. H., 1989. A review on solubility and polymerization of silica. Geothermics, Vol. 18, pp. 49-56.

Chen, C. T. A., and W. L. Marshall, 1982. Amorphous silica solubilities IV: Behavior in pure water and aqueous sodium chloride, and magnesium sulfate solutions up to *350°C.* Geochimica et Cosmochimica Acta, Vol. 46, pp. 279-287.

DiPippo, R., 1985. A simplified method for estimating the silica scaling potential in geothermal power plants. Geothermal Resources Council Bulletin, Vol. 14, May 1985, pp. 3-9.

Fournier, R.O., 1981. Application of water chemistry to geothermal exploration and reservoir engineering. In: L. Rybach and L. J. P. Muffler, eds., Geothermal Systems: Principles and Case Histories, Wiley, New York, pp. 109-143.

Fournier, R. O., 1985. The behavior of silica in hydrothermal solutions. In: B. R. Berger and P. M. Bethke, eds., Geology and Geochemistry of Epithermal Systems. Reviews in Economic Geology, Vol. 2., Society of Economic Geologists, p. 61.

Fournier, R. O., and W. L. Marshall, 1983. Calculation of amorphous silica solubilities at 25° to 300°C and apparent cation hydration numbers in aqueous salt solutions using the concept of effective density of water. Geochimica et Cosmochimica Acta, Vol. 47, pp. 587-596.

Fournier, R. O., and R. W. Potter, II, 1982. A revised and expanded silica (quartz) geothermometer. Geothermal Resources Council Bulletin, Vol. 11, November 1982, pp. 3-12.

Fournier, R. O., and J. J. Rowe, 1977. The solubility of amorphous silica in water at high temperatures and high pressures. American Mineralogist, Vol. 62, pp. 1052-1056.

Hauksson, T., and J. S. Gudmundsson, 1986. Silica deposition during injection in Svartsengi field. Geothermal Resources Council Transactions, Vol. 10, pp. 377-384.

Henley, R. W., 1983. pH and silica scaling control in geothermal field development. Geothermics, Vol. 12, pp. 307-331.

Henley, R. W., A. H. Truesdell, P. B. Barton, Jr., and J. A. Whitney, 1984. Fluid-mineral equilibria in hydrothermal systems. Society of Economic Geologists, Reviews in Economic Geology, Vol. 1.

Hibara, Y., M. Tahara, and S. Hidenori, 1989. Operating results and reinjection of Milos field in Greece. Geothermics, Vol. 18, pp. 129-135.

Hirowatari, K., and M. Yamaguchi, 1990. Experimental study on a scale prevention method using exhausted gases from geothermal power stations. Geothermal Resources Council Transactions, Vol. 14, Part II, August 1990, pp. 1599-1602.

Hurtado. R., and S. Mercado, 1990. Scale control studies at the Cerro Prieto geothermal field. Geothermal Resources Council Transactions, Vol. 14, Part II, August 1990, pp. 1603-1610.

Iler, R. K., 1979. The Chemistry of Silica-Solubility, Polymerization. Colloid and Surface Properties, and Biochemistry. John Wiley & Sons, Inc., New York.

Itoi, R., M. Fukada, **K.** Jinno, **K.** Hirowatari, N. Shinohara and T. Tomita, 1989. Long-term experiments of waste water injection in the Otake geothermal field, Japan. Geothermics, Vol. 18, pp. 153-160.

Jamieson, R. E., 1984. Simulation of the silica scaling process. Proceedings of the 6th New Zealand Geothermal Workshop, University of Auckland Geothermal Institute, pp. 135-140.

Karabelas, A. J., N. Andritos, A. Mouza, M. Mitrakas, F. Vrouzi, and K. Christanis, 1989. Characteristics of scales from the Milos geothermal plant. Geothermics, Vol. 18, pp. 169-174.

Kindle, C. H., B. W. Mercer, R. P. Elmore, S. C. Blair and D. A. Myers, 1984. Geothermal injection treatment: process chemistry, field experiences and design options. Batelle Pacific Northwest Laboratory, PNL-4767 UC-66d.

Klein, C. W., S. Iwata, R. Takeuchi and T. Naka, 1991 Prediction and prevention of silica scaling at low levels of oversaturation: case studies and calculations for Ueaotai Geothermal Field, Akita Prefecture, Japan. Proceedings, Sixteenth Workshop on Geothermal Reservoir Engineering, Stanford University, California

Marsh, A. R. III, G. Klein, and **T.** Vermeulen, 1975. Polymerization kinetics and equilibria of silicic acid in aqueous solution. University of California Lawrence Berkeley Laboratory Report LBL-4415, October 1975.

Mroczek, **E.** K., and G. McDowell, 1990. Silica Scaling Field Experiments. Geothermal Resources Council Transactions, Vol. 14, Part II, August 1990, pp. 1619-1625.

Rothbaum, H. P., B. H. Anderson, R. F. Harrison, A. G. Rotde and A. Slatter, 1979. Effect of silica polymerization and pH on geothermal scaling. Geothermics, Vol. 8, pp. 1-20.

Stock, D.D., 1990. The 'use of pressure drop measurements to monitor scale build-up in pipelines and wells. Geothermal Resources Council Transactions, Vol. 14, Part II, August 1990, pp. 1645-1651.

Thordarsson, H. and T. Tomasson, 1989. Brine clarification at Svartsengi, Iceland: Effect of pH and temperature on the precipitation of silica and its properties. Geothermics, Vol. 18, pp. 287-294.

Weres, O., **A.** Yee and L. Tsao, 1982. Equations and type curves for predicting the polymerization of amorphous silica in geothermal brine. Society of Petroleum Engineers Journal, Vol. 22, pp. 9-16.

APPENDIX A UENOTAI, JAPAN, WELL FLUID COMPOSITION

Total flow enthalpy 447.98 cal/gm
Water fraction at separation pressure 5.0 bar

Parameter	mg/l	Parameter	mg/l
Ca	0.39	Tot.Alk(as HCO_3)	56.08
Mg	0.04	SO_4	31.24
Na	180.50	Cl	247.56
K	37.14	SiO_2	892.27
Li	0.55	F	2.34
Cs	0.03	B	1.24
NH_4	0.42	H_2S	11.76
Al	1.38		
As	0.24	pH (lab.)	8.89/22°C
TDS(meas.)	1,374.06	Ion balance	
TDS(sum)	1,418.69	(difference/sum)	+1.29
TDS_m/TDS_s	0.969		

Gas fraction: at separation pressure 4.5 bar

Dry gas CO_2	83.98 vol.%	Gasisteam
H_2S	6.48	2,727. mm/1,000m
N_2	4.06	
CH_4	5.66	
H_2	4.94	

APPENDIX **B:** FLUID MODELING CALCULATIONS - **THE** SILICA PROBLEM

Fluid modeling for this report was done using a modified version of a thermodynamic speciation-solubility computer code (Amorsson and Sigurdsson, 1982). Equilibrium constants for silica species were taken from: Fournier and Potter, 1982 (quartz); Fournier and Rowe, 1977 (amorphous silica); Fournier, 1985 and personal communication (log K_{am}); and Arnorsson and Sigurdsson, 1982 (log K_{H3SiO4}, log $K_{NaH3SiO4}$). Codes of this type depend on a measurement of pH at some known temperature, along with the sample composition, as a basis for calculating pH at some new temperature, with or without recombination of volatilized gases, H_2O, precipitated/dissolved minerals, etc.. In essence, the codes relate measured pH to some pH-dependent parameter which can be calculated, such as a sum of weak acid ions or "total ionizable H". Then they calculate what the new value of this parameter should be at the new temperature, and iterate to find the pH which produces that value (see review in Henley *et al.*, 1984, chapter 7).

The correctness of pH calculations can be affected by a problem inherent in standard methods of sample analysis and data input to the computer codes. It is not clear from a literature survey how widely this problem has been considered, but it has been very relevant to calculations using the Appendix **A** fluid sample.

The problem is a mismatch between measured total SiO_2 and measured pH. The reported total SiO_2 has been measured by some technique (AA, colorimetry on a diluted sample) designed to determine all of the SiO_2 present in the water at the time of sample collection. pH is measured in a cooled sample, often several days after the sample was collected. The measured value is the result of a balance of numerous simultaneous chemical equilibria, which keep the sample in a natural state of charge balance. In a geothermal water sample, this process is dominated by carbonate species, silica species, sulfide species, boron species, ammonia species, ***et al.,*** with the silica species being particularly significant at pH above about 8. The computer code simulates this process, using the total SiO_2 measurement to calculate the contribution of the silica species equilibria. If the sample is oversaturated with respect to amorphous silica, the real concentration of SiO_2 which contributes to determining pH **is** less than the measured total, because some fraction of the total is trapped in suspended colloidal polymers. (The effect of this is buffered to some degree by the fact that the acidity of the polymers is higher than the acidity of monomeric SiO_2 (Marsh *et al.*, 1975). **As** far as we know, this is not quantified in any of the existing computer codes.) The result is that the codes may overestimate the contribution of silica species to the parameter which they use later to determine pH at some different temperature. The size and impact of the miscalculation increases with increasing oversaturation, and increasing ratio (silica species/carbonate species). The existence of the miscalculation becomes most apparent when the water is very dilute but has very high silica, as seen by comparing measured ion balance with speciated ion balance. For example, in the sample of table 1, the ion balance of species determined by analysis is +1.29%, but the speciated ion balance is greater than -12.5% (if all of the measured alkalinity is due to silica, and more negative if some alkalinity is due to carbonic acid species), because of the large amount of $H_3SiO_4^-$ calculated to be present.

For the sample of Appendix A, the overestimation results in calculating a reservoir pH (at 285°C) which is too high by as much as 0.4. This is seen by first calculating reservoir speciation using the measured pH and SiO_2. The result is pH 7.40/285°C.

Next, take the same sample, charge balance the analytical species with Cl, then adjust pH to get a speciated balance. The result (pH 8.111 22°C) is ideally the pH the sample would have had were all SiO_2 present in monomeric form. Using it as input, reservoir speciation gives pH 7.0/285°C.

This adjustment procedure is risky because of sensitivity to analytical errors, but for the Appendix A sample it seemed likely to give more valid estimates of pH in the reservoir and various steam separation conditions than using the measured pH value.